Environmental Science: Atmospheres

ROYAL SOCIETY OF CHEMISTRY

PAPER

View Article Online
View Journal | View Issue



Cite this: *Environ. Sci.: Atmos.*, 2023, **3**, 1778

# $NO_3$ reactivity measurements in an indoor environment: a pilot study†

Patrick Dewald, Jos Lelieveld and John N. Crowley *

We present the first direct indoor measurements of VOC-induced nitrate radical ($NO_3$) reactivity ($k^{NO_3}$) together with measurements of nitric oxide (NO), nitrogen dioxide ($NO_2$), ozone ($O_3$) and dinitrogen pentoxide ($N_2O_5$) inside a laboratory during a four-day period in October 2021 in a suburban area (Mainz, Germany). Indoor mixing ratios of $O_3$ ranged from <2–28 ppbv and those of $NO_2$ from 4.5–27 ppbv. The rapid ventilation of the room (air change rates of ~4 $h^{-1}$) meant that indoor mixing ratios mirrored the variability in $NO_2$ and $O_3$ outdoors. $NO_3$ production rates were between <0.02 and 0.12 pptv $s^{-1}$ with indoor $N_2O_5$ mixing ratios increasing to 4–29 pptv during five NO-depleted day- or nighttime periods when $k^{NO_3}$ was between 0.04 and 0.2 $s^{-1}$. Steady-state calculations resulted in a peak $NO_3$ mixing ratio of 6 pptv. A comparison of measured $N_2O_5$ mixing ratios to those derived from steady-state calculations and the equilibrium coefficient for the $NO_2$, $NO_3$, $N_2O_5$ system showed very good agreement, indicating that heterogeneous reactions do not contribute significantly to the overall $NO_3$ loss rate ($L_{NO_3}$). During these five periods, $NO_3$ was mostly lost to NO and VOCs, the latter contributing on average 65% to $L_{NO_3}$. This pilot study underlines the necessity of further indoor $NO_3$ reactivity measurements and that the nitrate radical can be a significant indoor oxidizing agent when the room is sufficiently ventilated during episodes of moderate outdoor air pollution.

Received 13th September 2023
Accepted 3rd November 2023

DOI: 10.1039/d3ea00137g

rsc.li/esatmospheres



### Environmental significance

The nitrate radical ($NO_3$), formed by the reaction between ozone ($O_3$) and nitrogen oxide ($NO_2$), is an important nocturnal oxidant of unsaturated volatile organic compounds in the atmosphere. While its effect on the atmospheric lifetime of NO*x* has been extensively studied outdoors, indoor studies of $NO_3$ are very limited. The short atmospheric lifetime of $NO_3$ makes its detection challenging. We demonstrate the first direct measurement of $NO_3$ reactivity indoors, providing an alternative way to assess $NO_3$ concentrations under polluted conditions. Our measurements suggest that $NO_3$ can be the dominant indoor oxidant of limonene, which is often released indoors owing to its presence in cleaning agents. This study emphasizes that $NO_3$ chemistry can significantly impact indoor air quality.

## 1 Introduction

Since a great fraction of human lifetime is spent indoors, the composition of indoor air can have a significant impact on human health.[1] Analogous to outdoor environments, the major indoor oxidants are ozone ($O_3$), the hydroxyl radical (OH) and the nitrate radical ($NO_3$).[2–5] $NO_3$ is produced by the oxidation of nitrogen dioxide ($NO_2$) by ozone ($O_3$), both of which are usually present in indoor air from ventilation of outside air:[4]

$$NO_2 + O_3 \rightarrow NO_3 + O_2 \quad (R1)$$

Dinitrogen pentoxide ($N_2O_5$) is formed *via* reaction of $NO_3$ and $NO_2$ and is in thermal equilibrium with both:[6]

$$NO_3 + NO_2 + M \rightarrow N_2O_5 + M \quad (R2)$$

$$N_2O_5 + M \rightarrow NO_3 + NO_2 + M \quad (R3)$$

In outdoor environments during the day, $NO_3$ is removed rapidly by reaction with NO (R4) and *via* photolysis by sunlight ((R5a) and (R5b)).[7]

$$NO_3 + NO \rightarrow 2\ NO_2 \quad (R4)$$

$$NO_3 + h\nu\ (\lambda \approx 400 - 640\ nm) \rightarrow NO_2 + O \quad (R5a)$$

$$NO_3 + h\nu\ (\lambda \approx 585 - 640\ nm) \rightarrow NO + O_2 \quad (R5b)$$

$NO_3$ photolysis rates indoors are sufficiently diminished compared to outside so that (R5a) and (R5b) can be neglected and $NO_3$ gains in importance, relative to $O_3$ and OH, as an oxidizing agent.[4,10,11] As evident from (R1), $NO_3$ production (and its subsequent chemistry) relies on the presence of $O_3$ and $NO_2$. Elevated indoor ozone (and $NO_x$) levels are particularly common in urban buildings equipped with ventilation systems or when

*Department of Atmospheric Chemistry, Max-Planck-Institute for Chemistry, 55128 Mainz, Germany. E-mail: john.crowley@mpic.de*

† Electronic supplementary information (ESI) available. See DOI: https://doi.org/10.1039/d3ea00137g

windows are open,[12,13] so that indoor $NO_3$ production rates become significant. Indoor ozone can be consumed by NO (R6) in poorly ventilated, residential environments,[14] where a major (indoor) source of NO is gas cooking.[4]

$$NO + O_3 \rightarrow NO_2 + O_2 \quad (R6)$$

Unsaturated volatile organic compounds (VOCs) such as terpenes, which are highly reactive towards $NO_3$,[15] are often abundant in indoor environments as they are present in detergents and cleaning agents.[16] In some environments (*e.g.* forested regions), reactions with unsaturated hydrocarbons not only become the dominant $NO_3$ removal process at night, but even compete with (R4), (R5a) and (R5b) during the day.[8,9] In addition, the reaction of $NO_3$ with VOCs (R7) leads (among other products) to the formation of alkyl nitrates ($RONO_2$) or nitric acid ($HNO_3$), which, in outdoor environments can transfer to the particle phase leading to secondary organic aerosols (SOA) and/or particulate nitrate.[17,18]

$$NO_3 + VOCs\ (+O_2) \rightarrow\rightarrow \text{products } (e.g.\ RONO_2,\ HNO_3) \quad (R7)$$

While the impact of $O_3$ and OH on indoor air quality has been extensively investigated,[3,14,19,20] the number of studies examining the role of the nitrate radical in indoor environments is very limited. Along with some model calculations and steady-state calculations which suggest that indoor $NO_3$ levels are below 0.04 parts per trillion by volume (pptv),[13,21–24] only a few direct measurements of $NO_3$ or its equilibrium partner $N_2O_5$ are available.[25–27] Arata *et al.*[26] detected several pptv of $NO_3$ in a poorly-ventilated residential kitchen when the $NO_3$ production rate was artificially enhanced by continuous addition of "synthetic" $O_3$ (up to 40 parts per billion by volume, ppbv). Detectable mixing ratios of $N_2O_5$ and $NO_3$ in the lower pptv range have been reported for ventilated rooms (exchange rates of 3.8 $h^{-1}$ and 7 $h^{-1}$) in an office building and an athletic facility.[25,27]

This limited number of studies indicates that, in poorly ventilated rooms, high $NO_3$ loss rates make it difficult to assess the impact of the nitrate radical yet no direct indoor $NO_3$ reactivity measurements have been reported. In addition, with the outbreak of the COVID-19 pandemic, rapid ventilation of indoor environments has become increasingly important to reduce viral loads.[28,29] Rapid ventilation of outside air results in the transport of photochemically generated $O_3$ and $NO_x$ into the indoor environment. Clearly, indoor measurement of $NO_3$ mixing ratios, $NO_3$ production rates and $NO_3$ reactivity would thus help to assess the fate of $NO_3$ radicals in such an environment. In this study, we report the first measurements of VOC-induced $NO_3$-reactivity along with mixing ratios of the nitrogen oxides NO, $NO_2$, $NO_3$ and $N_2O_5$ together with $O_3$ from a well-ventilated laboratory over a weekend period in October 2021 in Mainz (Germany). Quantifying VOC-induced $NO_3$ reactivity together with the above-mentioned set of measurements enables identification of the dominant $NO_3$ loss processes which may allow qualitative conclusions about the formation of organic nitrates indoors to be drawn. The purpose of this study is thus to evaluate whether $NO_3$ reactivity measurements provide us with new insights into indoor oxidation processes.

## 2 Experimental

The laboratory used in this study has a volume of ~220 $m^3$ (floor area = 61 $m^2$) and was mostly unoccupied during the measurement period in order to reduce the impact of the human emissions on the observations. The room itself is located at the Max-Planck-Institute for Chemistry (MPIC) that is situated in direct vicinity to commercial, residential and university buildings. Busy two- and four-lane roads leading to the city center of Mainz (5 km, 217 000 inhabitants) are adjacent to the institute. Mainz is part of the densely populated and industrialized Rhine-Main area close to Frankfurt and Wiesbaden. A ventilation system, that was continuously operated in "night-mode" (*i.e.* reduced air change rate, see Supplement S1†) during the study period constantly replenished the room with urban (polluted) air from outside. The air change rate ($k_{change}$) was estimated using a tracer-gas approach[30] in which limonene or 2,3-dimethyl-2-butene was released into the laboratory and its decay in concentration was monitored. The concentration of limonene or 2,3-dimethyl-2-butene was not measured directly but by the change (reduction) in $NO_3$ reactivity as their mixing ratios decreased mainly due to exchange with outdoor air. Following a phase of mixing (<1 min) initial concentrations of ≈ 200 pptv (for limonene) decrease to roughly zero in ≈ 30 min. The decay of limonene and of 2,3-dimethyl-2-butene is exponential, enabling decay constants (or air change rate constants) of 5.76 $h^{-1}$ (limonene) and 4.3 $h^{-1}$ (2,3-dimethyl-2-butene) to be derived. The faster decay term for limonene is likely related to its indoor oxidation and wall loss, which are both expected to be more rapid than for 2,3-dimethyl-2-butene. Due to the bias caused by deposition and chemical loss processes, the values derived by our approach serve as an upper limit of the true air change rate. In the case of limonene, gas-phase losses contribute ≈ 30% to the overall decay rate. The air change rate of our laboratory during the measurement period was less than 4 $h^{-1}$. The procedure and results of the air change rate determination are found in more detail in the Supplement (S1†). Note that a more volatile and less reactive tracer such as carbon dioxide ($CO_2$), which is readily available through respiration and can be detected by inexpensive sensors, represents an alternative tracer.

The east side of the room featured windows to an inner courtyard. Light entering the room through the permanently closed windows was attenuated by a fine-meshed sunscreen. The room lights (fluorescent strip-lamps) were turned off during the entire period. Spectral-radiometric measurements verified that $NO_3$ photolysis rates ($J_{NO_3}$) resulting from the attenuated daylight (<$10^{-6}$ $s^{-1}$) were insignificant (see Supplement, Fig. S2†).

The laboratory was equipped with four instruments described below, each one connected to a central exhaust system. The NO bottles used to run the cavity ring-down spectrometers (CRDS) were stored in a separate, ventilated safety cabinet. All gas lines were thoroughly checked for leakages. By

avoiding potential laboratory (chemical) emissions, the composition of the air should thus be comparable to other ventilated rooms. The measurements were carried out at the institute during a four-day period from Friday to Tuesday in October 2021 during which the maximum outdoor daytime and nighttime temperatures were 14 °C and 5 °C, respectively. The weather during the weekend was dominated by clouds and fog, the only extended sunny period was on October 16 between 07:00 and 15:00 UTC.

### 2.1 $NO_3$ reactivity

The $NO_3$ reactivity ($k^{NO_3}$) was directly measured with a cavity ring-down spectrometer that was coupled to a flowtube (FT-CRDS) as detailed in Liebmann *et al.*[31] After accounting for the impact of $NO_x$ (see below), this instrument quantifies the total gas-phase $NO_3$ reactivity (*i.e.* the inverse of the $NO_3$ lifetime) towards VOCs, so that $k^{NO_3}$ is equal to the summed first-order loss rate $\Sigma k_i[VOC]_i$ with the concentration of a VOC $[VOC]_i$ and the corresponding rate coefficient $k_i$ for its reaction with $NO_3$ (R7). A commercial zero-air generator (CAP 180, Fuhr GmbH) provides 400 standard (STP) cubic centimeters per minute (sccm) of zero-air which is passed over a mercury lamp (Penray) to generate $O_3$ at *ca.* 400 ppbv. This flow is mixed with a flow of NO (3 sccm of 1 parts per million by volume (ppmv) in $N_2$, Air Liquide) and directed through a thermostated Teflon-coated (FEPD 121, Chemours) reactor (30 °C, 1.3 bar). During the residence time of *ca.* 5 min, $O_3$ sequentially oxidizes NO to $NO_2$ (R5) and then to $NO_3$ (R1), which reacts with $NO_2$ to form $N_2O_5$ (R2). Passing the gas through a 15 cm long piece of PFA (perfluoroalkoxy) tubing (outer diameter (OD) of 1/4 in. = 0.635 cm) heated to 140 °C converts $N_2O_5$ to $NO_3$ and $NO_2$ (R3). The flow containing $NO_3$ is then mixed with 2800 sccm synthetic or ambient air and directed through a Teflon-coated (FEPD 121, Chemours) flowtube, where the gas-mixture has a time of 11 s to react. The $NO_3$ that survives the flowtube is quantified using cavity ring-down spectroscopy (CRDS) at a wavelength of 662 nm. The basic principle of the instrument thus relies on comparing the level of synthetic $NO_3$ in zero-air (*i.e.* total $NO_3$ reactivity = 0 $s^{-1}$), to those in indoor air. The ring-down time in the absence of $NO_3$ was determined by the periodic addition of sufficient NO (3 sccm of 100 ppmv NO in $N_2$, Air Liquide) to titrate the $NO_3$ completely. Zero-air was humidified to match indoor-air humidity using a permeation-tube based humidification system (PermaPure, MH-070-24F-4) filled with deionized water (LiChrosolv, Merck). Indoor air was sampled through 1 m 1/4 in. (OD) PFA tubing equipped with a Teflon membrane filter (Pall Corp., 47 mm, 0.2 μm pore) to protect the mirrors and through a 2 L (uncoated) borosilicate glass flask heated to 45 °C to remove both ambient $NO_3$ and $N_2O_5$, which would bias the measurement.

Indoor air was dynamically diluted with zero-air during periods with highly reactive ambient air, which extends the upper limit of measurable reactivities to 1.7 $s^{-1}$. The variability of the $NO_3$ source and cavity instabilities results in a lower limit of detection (LOD) of 0.006 $s^{-1}$ and contribute ~18% to the measurement uncertainty.

As described by Liebmann *et al.*,[31] the presence of NO, $NO_2$, $O_3$ (and thus reactions ((R1–R4) and (R6) and (R7)) and $NO_3$ losses on the walls of the flowtube ($NO_3$ wall loss rate = 0.001 $s^{-1}$) require numerical simulations in order to extract the $NO_3$ reactivity ($k^{NO_3}$) that can be attributed to VOCs (R7). Due to the numerical correction procedure, the total uncertainty of the measurement is dependent on the ratio of ambient $NO_2$ and $k^{NO_3}$.[31] Note that conversion of NO to additional $NO_2$ *via* (R6) in the flowtube affects $NO_2/k^{NO_3}$ which is why accounting for the impact of NO becomes significant in polluted conditions not only because of (R4). If, for example, a reactivity of 0.15 $s^{-1}$ is measured in the presence of 12 ppbv $NO_2$, the additional uncertainty introduced by the numerical simulations would be ~24%, leading to a total measurement uncertainty (TMU) of 30% which corresponds to the median TMU of this instrument during the study.

### 2.2 $NO_3$ and $N_2O_5$

Ambient $NO_3$ and $N_2O_5$ mixing ratios were monitored using the two 662 nm cavities of the five-channel cavity ring-down spectrometer (5Ch-CRDS), described by Sobanski *et al.*[32] In this instrument, $N_2O_5$ is quantitatively dissociated to $NO_3$ (R3) by passing the sample air through a Teflon-coated glass tube heated to 95 °C prior to entering the cavity at the same temperature. The heated cavity consequently detects the sum of $NO_3 + N_2O_5$. Similar to the FT-CRDS, the "baseline" (*i.e.* the ring-down time in the absence of the absorbing species) was determined by adding NO to the cavity (6 sccm of 100 ppmv NO in $N_2$, Air Liquide). Air was sampled at 15 standard (STP) liters per minute (SLPM) through 10 cm of 1/4 in. (OD) PFA tubing and a Teflon membrane filter (Pall Corp., 47 mm, 0.2 μm pore) with the heated cavity sampling 7 SLPM and the unheated one 8 SLPM. To reduce $NO_3$ loss through the inlet, an automatic filter changer normally replaces the inlet filter every hour. Unfortunately, the filter changer was not available during the measurement period. The data was corrected for cavity losses of $NO_3$, the effective $NO_3$ cross-section at both cavity temperatures and the impact of the mirror purge gas flow as described in Sobanski *et al.*[32] Taking the standard deviation (2σ) from the baseline variability of the whole 10 min-averaged data set results in LODs of 0.9 pptv and 1.5 pptv for $NO_3$ and $N_2O_5$, respectively. The total uncertainty associated to the $NO_3$ and $N_2O_5$ measurements is 25% and 28%, respectively.

### 2.3 NO and $NO_2$

NO and $NO_2$ were measured with a two-channel, cavity ring-down spectrometer[33] operated at 405 nm. One cavity directly samples ambient air to detect $NO_2$, while the other samples *via* additional tubing (1 m 1/2 inch (OD) PFA) that forms a reaction volume in which NO is oxidized to $NO_2$ *via* the addition of ~3 ppmv $O_3$ (R6). The second cavity thus detects the sum of NO and $NO_2$ so that NO mixing ratios were derived by the difference signal. Each cavity sampled indoor air at a flow of 2 SLPM through ~2 m 1/2 in. (OD) PFA tubing and a Teflon membrane filter (Pall Corp., 47 mm, 0.2 μm pore). Based on the noise level and the variability in the baseline, the LODs of the NO and $NO_2$

measurements are 132 pptv and 57 pptv with associated uncertainties of 11% and 9%, respectively.

Since the correction of the $NO_3$ reactivity measurements requires accurate $NO_2$ measurements, $NO_2$ mixing ratios were additionally monitored with a cavity of the 5Ch-CRDS operated at 405 nm. A comparison of both $NO_2$ measurements is presented in the Supplement (Fig. S3†) and reveals excellent agreement between the two-channel and five-channel instruments. As both instruments were placed in opposed corners of the laboratory, this comparison also confirms that the air in the room is well mixed.

### 2.4 $O_3$ and other auxiliary measurements

Ozone mixing ratios were measured with a commercial ozone monitor (2B Technologies, model 205) based on UV absorption. The instruments detects $O_3$ mixing ratios > 2 ppbv with an uncertainty of 5%.

Relative humidity (RH) and temperature ($T$) measurements were monitored with the $NO_3$ reactivity setup (see 2.1) by separately sampling 500 sccm ambient air over a commercial hygrometer (Innovative Sensor Technology, HYT939) with an accuracy of ±1.8% (RH) and ±0.2 °C ($T$). Total (*i.e.* non-size-segregated) particle number densities were sporadically measured after the pilot study using a condensation particle counter (CPC, TSI, model 3025a).

Indoor photolysis frequencies were determined using a spectral-radiometer (Metcon GmbH) with a single monochromator and 512 pixel CCD array as a detector (275–640 nm). The thermostated monochromator-detector unit was attached *via* a 10 m optical fiber to an integrating hemispheric quartz dome that was placed at a height of *ca.* 2 m in the center of the room. Light fluxes were converted to photolysis rate constants for $NO_3$ ((R5a) and (R5b), $J_{NO_3}$) and $NO_2$ ($J_{NO_2}$) using molecular parameters recommended by the IUPAC and NASA evaluation panels.[34,35]

## 3 Results and discussion

A time-series of the mixing ratios of NO, $NO_2$, $O_3$, $NO_3$ and $N_2O_5$ as well as RH, $T$ and $k^{NO_3}$ is given in Fig. 1 together with calculated quantities (*e.g.* production and loss rates of $NO_3$) that are discussed in section 3.2. Within the measurement period, the relative humidity varied between 24% and 36% at a fairly constant temperature of 297–298 K (panel a). NO (<132 pptv to 41 ppbv, panel b), $NO_2$ (4.5 to 27 ppbv, panel b) and $O_3$ (<2 ppbv to 28 ppbv, panel c) mixing ratios were quite variable. During

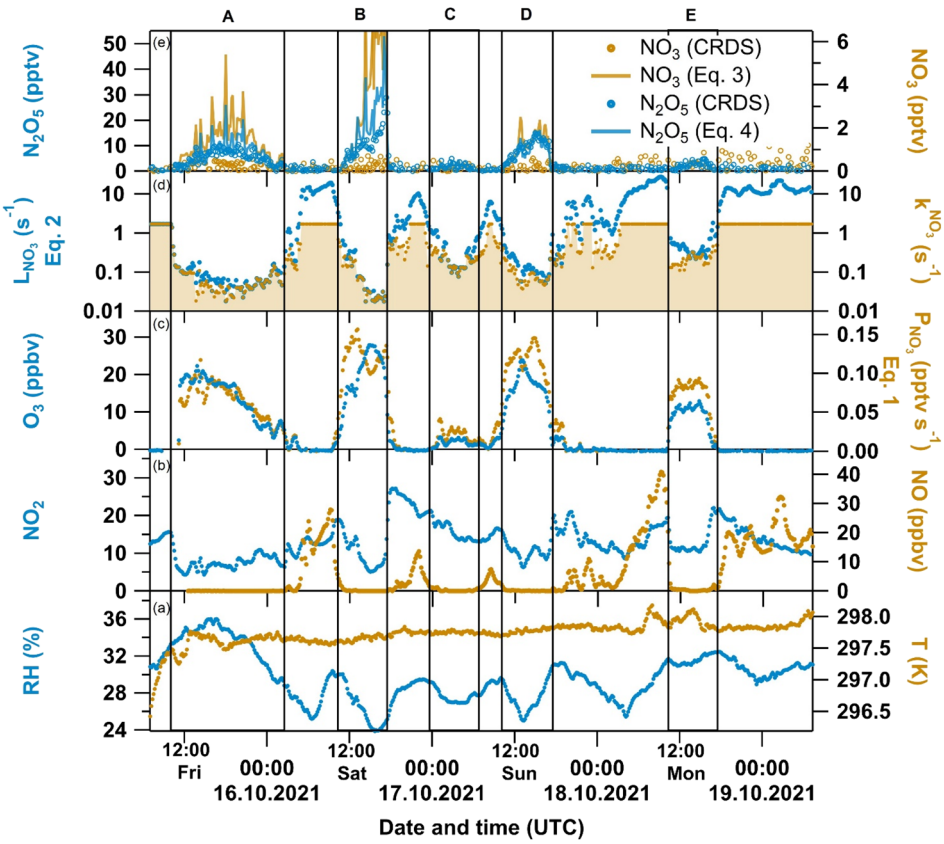


Fig. 1 Overview of directly measured and derived quantities during a weekend period inside a ventilated laboratory: (a) relative humidity RH (blue, left axis) and temperature $T$ (orange, right axis); (b) $NO_2$ (blue, left axis) and NO (orange, right axis) (c) $O_3$ (blue, left axis) and $NO_3$ production rate $P_{NO_3}$ from (Eq. 1) (blue, right axis); (d) Total $NO_3$ loss rate $L_{NO_3}$ from (Eq. 2) (blue, left axis) and $NO_3$ reactivity $k^{NO_3}$ (LOD of 1.7 $s^{-1}$, orange with same-coloured shaded area to mark its contribution to $L_{NO_3}$); (e) $N_2O_5$ (blue circles, left axis), calculated $N_2O_5$ from (Eq. 4) (blue line, left axis), $NO_3$ (orange circles, right axis) and calculated $NO_3$ from (Eq. 3) (orange line, right axis).

the periods in which NO was high, likely a result of nearby automobile emissions, the $NO_3$ reactivity exceeded the instrument's upper LOD of 1.7 $s^{-1}$ (panel d), which was reached when the NO mixing ratio exceeded 2.5 ppbv.

We have divided the measurements into five periods (A–E in Fig. 1), during which $N_2O_5$ mixing ratios (panel e) were >2 pptv and NO mixing ratios were close to or below the LOD, whereas $O_3$ mixing ratios were large. The anti-correlation between NO and $O_3$ is readily understood considering the efficient conversion of NO to $NO_2$ *via* (R6), which has the following consequences: (1) The presence of $O_3$ (together with $NO_2$) enables the production of both $NO_3$ and $N_2O_5$. (2) The lack of NO leads to lower $NO_3$ reactivities (*i.e.* higher $NO_3$ lifetimes) of between 0.04 to 0.2 $s^{-1}$. This is reflected in measurable amounts of $N_2O_5$ (up to 29 pptv) during period B.

In this study, $NO_3$ remained undetected. Considering the thermal equilibrium between $NO_2$, $NO_3$ and $N_2O_5$ ((R2) and (R3)) and the measured $NO_2$ and $N_2O_5$ mixing ratios, this is contradictory to calculations using evaluated rate coefficients for $k_2$ and $k_3$,[35] which indicated the presence of 2–4 pptv $NO_3$. The most likely explanation is that $NO_3$ (a reactive radical) was lost during sampling through the inlet tubing and filter, while both $N_2O_5$ and $NO_2$ pass almost loss-free through the system. After use over the 4 days period, the inlet filter was clearly contaminated with dark-coloured particles, presumably black-carbon. A picture of this filter in comparison to an unused filter is shown in the Supplement (Fig. S4†). A previous study[36] on the interaction of $NO_3$ and $N_2O_5$ with urban aerosols collected on filter samples at the same location showed no measurable uptake for $N_2O_5$, whereas $NO_3$ was lost efficiently with $\gamma(NO_3)/\gamma(N_2O_5) > 15$, where $\gamma$ is the net-uptake coefficient for heterogeneous loss.

Outdoors, $NO_3$ and $N_2O_5$ are usually only observed during nighttime due to $NO_3$ photolysis rates of typically up to 0.17 $s^{-1}$ at noon,[7] whereas in this study $N_2O_5$ was detected independently of the diel cycle. In Fig. 1, period A covers a daytime–nighttime transition, the $N_2O_5$ peaks in periods B, D and E are around noontime, while period C is a nighttime period. However, an air change rate of 4 $h^{-1}$ is sufficient to entrain $N_2O_5$ originating from outside into the laboratory especially at night. To assess the potential impact of outdoor $N_2O_5$ on our measurement, we compare the calculated *in situ* indoor $N_2O_5$ production rate $P_{indoor}(N_2O_5)$ with the production rate $P_{outdoor}(N_2O_5)$ caused by infiltration of $N_2O_5$ originating from outside. According to (R2) and (Eq. 4), $P_{indoor}(N_2O_5)$ is equal to $k_2[NO_2][NO_3] \approx k_1k_2[NO_2]^2[O_3]/L_{NO_3}$. Calculation of $P_{indoor}(N_2O_5)$ from our measurements of $NO_2$, $O_3$, NO and $k^{NO_3}$ results in values of 0.1–2.1 pptv $s^{-1}$ during periods A–E. Schuster *et al.*[37] reported nighttime $N_2O_5$ mixing ratios outside the institute in October 2007 of up to 80 pptv which would result in an production rate $P_{outdoor}(N_2O_5) = [N_2O_5]_{outdoor} \times k_{change}$ of $\approx$ 0.01 pptv $s^{-1}$. Unless several hundreds of pptv of $N_2O_5$ were constantly abundant outside, $P_{outdoor}(N_2O_5)$ is very unlikely to affect our $N_2O_5$ levels measured inside.

### 3.1 Comparison of indoor and outside air

With an air change rate of up to 4 $h^{-1}$, the composition of the air in the laboratory is strongly influenced by that outside. Fig. 2 compares the indoor mixing ratios of $O_3$ and $NO_2$ to those from a local air-quality measurement station[38] located in Mainz-Mombach, *ca.* 4 km north of the Max-Planck-Institute. For both trace gases, the indoor/outdoor diel profiles are very similar. Outdoor $O_3$ is close to zero at nighttime, which is the result of deposition to surfaces and also reaction with NO forming $NO_2$ (R6). Outdoors, $NO_2$ is rapidly photolysed during the day (R8) to re-generate $O_3$ (R9), whereas indoor photolysis rates for $NO_2$ ($J_{NO_2}$) are very low (see Fig. S2 in the Supplement†) and there are no significant *in situ* sources of $O_3$ in the laboratory. The availability of $O_3$ indoors thus depends entirely on exchange with outdoor air and the strong co-variance is expected. Outdoors, the nighttime increase in $NO_2$ (resulting from the oxidation of locally emitted NO) results in rapid formation of $O_3$ at the start of the day as $NO_2$ is photolysed (to $O(^3P)$ and thus $O_3$).

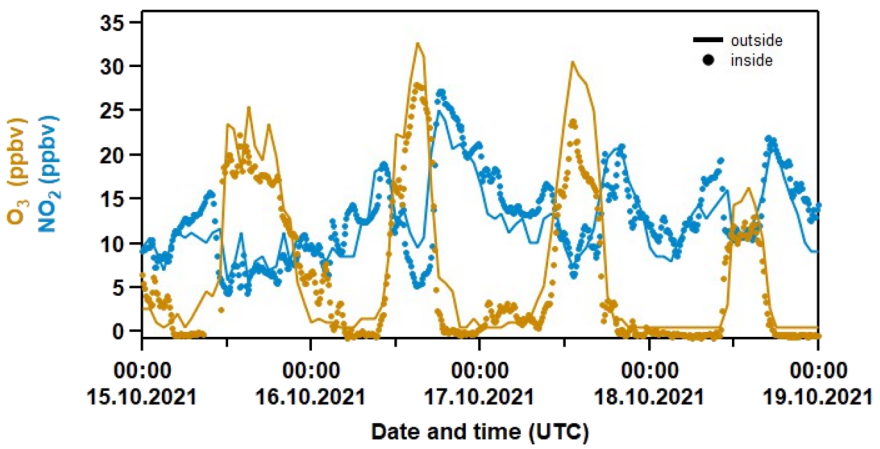


Fig. 2 Measurements of $O_3$ and $NO_2$ inside the laboratory (dots, 10 min data) and outside at a station in Mainz–Mombach (solid line, 1 h data). The outdoor data was taken from the German Environment Agency[38] and converted from μg $cm^{-3}$ to ppbv using a pressure of 760 Torr and a temperature of 298 K.

$$NO_2 + h\nu \rightarrow NO + O(^3P) \quad \text{(R8)}$$

$$O(^3P) + O_2 + M \rightarrow O_3 + M \quad \text{(R9)}$$

There is no obvious lag in the indoor $O_3$ data at sunrise compared to outdoors, which implies that the air change rate is more rapid than the production and loss terms for $O_3$. The indoor-to-outdoor ratio (I/O) of $O_3$ and $NO_2$ was obtained by measuring both $NO_2$ and $O_3$ sequentially inside the laboratory and directly outside by passing the inlet through a port in the wall (Fig. 3). In this case, I/O($O_3$) was determined to be 0.63 ± 0.03 (1σ). Note that windows are shut at all times in the laboratory, and that outdoor air passes through a compressor, metal piping and filters before entering the labs so $O_3$ is expected to be lost, which explains the lower than unity indoor/outdoor ratio. An average I/O of 0.25 was recently reported in a review summarizing measurements in *ca.* 2000 indoor environments.[14]

I/O($O_3$) can be assessed by assuming that the air change rate $k_{change}$ and surface removal rate $k_{surface}$ of $O_3$ are much faster than its outdoor variability so that I/O($O_3$) = $k_{change}/(k_{change} + k_{surface})$.[12] Using an air change rate of 4 $h^{-1}$ and a surface removal rate for $O_3$ as reported for a laboratory environment of 2.5 $h^{-1}$,[12] I/O($O_3$) = 0.62 is derived, which is close to the observed value. However, I/O($O_3$) is affected by several parameters such as the air change rate, abundance of NO, loss rate on indoor surfaces (highly dependent on the material), transmission loss through ventilation systems and the presence of humans.[14] The values of $k_{surface}$ may consequently be very different for two non-identical laboratories. Since indoor $O_3$ only reached elevated levels when NO ≤ 150 pptv resulting in a maximum $O_3$ loss rate of 0.25 $h^{-1}$, the contribution of (R6) was neglected.

As mentioned above, the oxidation of NO by $O_3$ not only leads to $O_3$ loss, but also to formation of $NO_2$. As shown in Fig. 3, the indoor mixing ratios of $NO_2$ (1800–2100 pptv) were indeed higher than outside (1100 to 1700 pptv). The high variability in $NO_2$ outside makes it impossible to accurately quantify a value for I/O($NO_2$), which is highly dependent on the availability of indoor $NO_2$ sources, the ratio between $k_{change}$ + $k_{surface}$ (similarly to $O_3$), season (photochemistry) and location. Models and long-term experiments show that I/O($NO_2$) is often above or close to unity in non-domestic, strongly ventilated rooms in urban areas similar to our laboratory.[39,40]

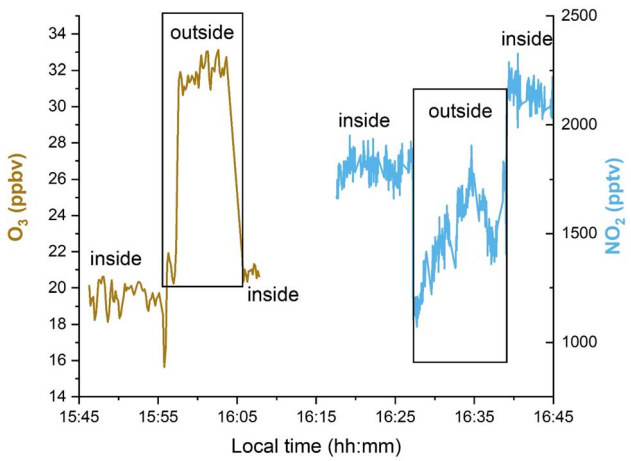


Fig. 3 Sequential measurements of $O_3$ and $NO_2$ inside and outside the laboratory on the 21st October 2021.

In summary, Fig. 2 and 3 underline (1) that (for a given ventilation rate) the indoor abundance of the $NO_3$ precursors ($NO_2$ and $O_3$) are mainly determined by the air composition outside and (2) that (R6), similarly to outdoors, explains the distinct anti-correlation between $O_3$ and $NO_x$ measured indoors as observed in Fig. 1.

In this laboratory environment, in which the indoor air is supplied by a compressor/filter system, the particle concentration is greatly reduced compared to outdoors. A few checks (after our pilot study) showed that the typical number density indoor-to-outdoor ratio, I/O($N_{part}$), was close to 0.1. As shown below, the low particle number density results in low aerosol surface areas, hence leading to insignificant losses of *e.g.* $N_2O_5$ or $NO_3$ to particles in ambient air compared to other surfaces and/or reactants. Nevertheless, accumulation of ambient particles on our inlet filter with time results in quantitative $NO_3$ removal prior to entering our cavity.[36] The PTFE membrane filters are usually changed (automatically) on an hourly basis during measurements to avoid this issue.[32,41]

### 3.2 Measured *versus* calculated $NO_3$ and $N_2O_5$ mixing ratios

$NO_3$ and $N_2O_5$ mixing ratios can be calculated from a stationary-state approximation if measurements of $NO_2$ and $O_3$ mixing ratios as well as $NO_3$ reactivity are available:[41–47] By using the rate coefficient $k_1$ for the reaction between $NO_2$ and $O_3$ (R1) and the mixing ratios of $O_3$ and $NO_2$, the $NO_3$ production rate ($P_{NO_3}$) can be assessed:

$$P_{NO_3} = k_1[NO_2][O_3] \quad \text{(Eq. 1)}$$

In our analysis, the $NO_3$ reactivity $k^{NO_3}$ is corrected for the impact of $NO_x$. Thus, in order to derive the overall $NO_3$ loss rate $L_{NO_3}$ (assuming only the overall gas-phase loss rate $k_{gas}$ is relevant compared to heterogeneous loss rate $k_{het}$), the pseudo-first-order loss rate constant for reaction with NO has to be added:

$$L_{NO_3} = k_{gas} + k_{het} \approx k^{NO_3} + k_4[NO], \quad \text{(Eq. 2)}$$

With $k_4$ being the rate coefficient for the reaction between NO and $NO_3$ (R4). In stationary state, *i.e.* $d[NO_3]/dt \approx 0$ the $NO_3$ loss rate is in balance with its production rate (Eq. 3) and its steady-state concentration $[NO_3]_{ss}$ can be calculated:

$$[NO_3]_{ss} = \frac{P_{NO_3}}{L_{NO_3}} = \frac{k_1[NO_2][O_3]}{k^{NO_3} + k_4[NO]} \quad \text{(Eq. 3)}$$

This approximation is valid as long as the system is in equilibrium ((R2) and (R3)), $NO_3$ loss rates are sufficiently large and $NO_2$ does not vary too much on short time-scales.[48,49] The thermal equilibrium constant $K_{eq} = k_2/k_3$ (ref. 35) enables derivation of $N_2O_5$ mixing ratios:

$$[N_2O_5]_{eq} = K_{eq}[NO_2][NO_3]_{ss} \quad \text{(Eq. 4)}$$

The $NO_3$ production and loss rates, and steady-state mixing ratios of $NO_3$ and $N_2O_5$ calculated using (Eq. 1) to (Eq. 4) are displayed in Fig. 1. When both $O_3$ and $NO_2$ were present (*i.e.* when $O_3$ was not removed by NO) the $NO_3$ production rates were between 0.02 and 0.12 pptv $s^{-1}$. Since the abundance of $O_3$ was the limiting factor in $NO_3$ production in this study, $P_{NO_3}$ mostly follows the diel pattern of $O_3$ (Fig. 1, panel c). During NO-rich periods, $O_3$ is not only entirely depleted (so that $P_{NO_3} \approx 0$ pptv $s^{-1}$), but $L_{NO_3}$ also increases to 10 $s^{-1}$ (panel d), which is why neither $NO_3$ nor $N_2O_5$ was expected. Furthermore, Fig. 1 (panel e) shows good agreement between measured and calculated $N_2O_5$ mixing ratios. At higher $N_2O_5$ mixing ratios, up to 6 pptv of $NO_3$ would have been present at equilibrium (with $NO_2$ and $N_2O_5$), which would have been detectable by our instrument. The lack of a $NO_3$ signal is attributed to its loss on a contaminated filter (see above).

In order to analyze the conditions under which indoor $N_2O_5$ is observable, we focus on period D (Fig. 4) which we consider representative of all periods in which $N_2O_5$ was detected. The uncertainties in $P_{NO_3}$, $L_{NO_3}$, $[NO_3]_{ss}$ and $[N_2O_5]_{eq}$ were derived from propagation of the uncertainties associated with the measurements (see section 2) as well as with the rate coefficients $k_1$ (15%) and $K_{eq}$ (20%).[34,35] In Fig. 4, $N_2O_5$ (panel e) starts to increase around 10:00 UTC and $O_3$ mixing ratios (panel c) increase from < 2 ppbv to 20 ppbv (at 14:00). At the same time, NO (panel b) decreases from 3 ppbv to close to, or below the LOD so that $NO_3$ loss rates (panel d) are around 0.04–0.1 $s^{-1}$. The $NO_3$ production rate (panel c) of *ca.* 0.06 pptv $s^{-1}$ (circa 20 ppb $O_3$ and 10 ppbv $NO_2$) is sufficient to generate detectable amounts of $NO_3/N_2O_5$ (panel e). These observations emphasize that the presence of $N_2O_5$ (and $NO_3$) goes hand-in-hand with $O_3$ mixing ratios that are sufficient for removal of NO (and its subsequent conversion to $NO_2$). As indicated in section 3.1, the abundance of indoor $NO_2$ and $O_3$ is mostly determined by their outdoor mixing ratios and the air change rate. Between 14:00 and 16:00 UTC in Fig. 4, we have 2 pptv $NO_3$ and 20 ppbv $O_3$. If we assume an OH concentration of $7 \times 10^5$ molecules $cm^{-3}$,[20,50] the loss rate constants for an indoor VOC such as limonene would be $5.91 \times 10^{-4}$ $s^{-1}$ ($NO_3$ loss), $1.08 \times 10^{-4}$ $s^{-1}$ ($O_3$ loss) and $1.15 \times 10^{-4}$ $s^{-1}$ (OH loss). During period D, $NO_3$ is thus the major oxidant of limonene and presumably other unsaturated compounds that display similar reactivity to $NO_3$. In contrast to the reaction with $O_3$ and OH which form carbonyl compounds (*e.g.* limona ketone, 4-acetyl-1-methyl-1-cyclohexene) and peroxy acetyl nitrate ($CH_3C(O)O_2NO_2$, PAN) indoors,[51] the $NO_3$-initiated oxidation of limonene results in the formation of alkyl nitrates ($RONO_2$) in high yields (30–67%).[35] Note that the reaction with $NO_3$ would only contribute *ca.* 30% to the total VOC loss rate when the maximum air change rate of 4 $h^{-1}$ is taken into account.

The good agreement between the measured and calculated $N_2O_5$ mixing ratios (Fig. 4) is further examined in Fig. 5 in which these quantities are plotted against each other. For this, mixing ratios at or below the LOD have been removed. A bivariate,

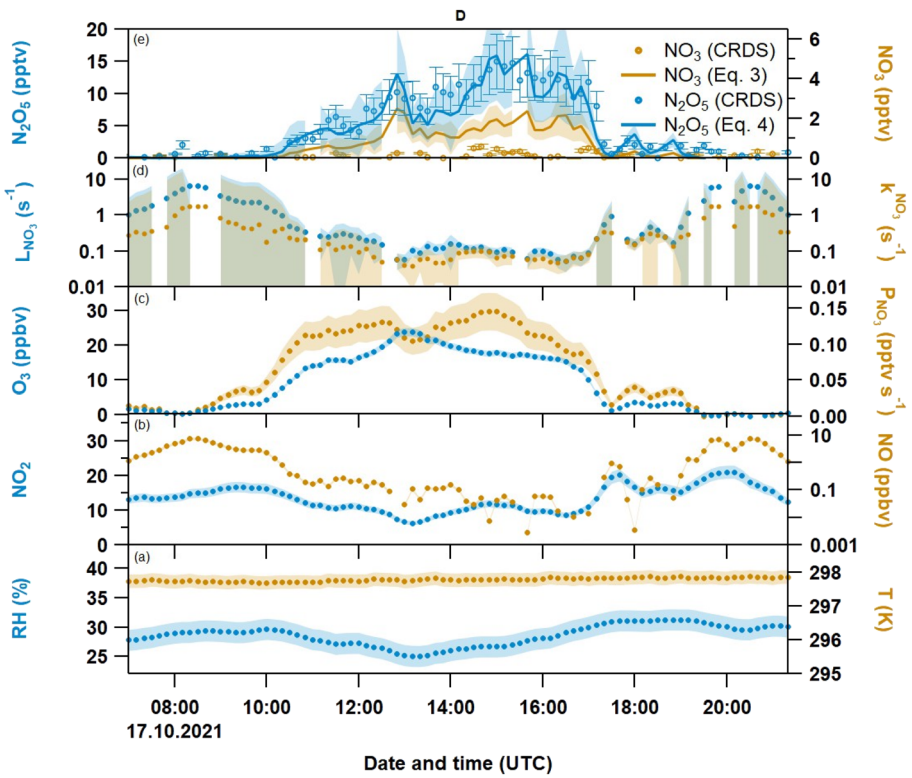


Fig. 4 Same as Fig. 1, but expanded to display period D. Total uncertainties are shown by shaded areas in the same color as the corresponding traces. In the case of directly measured $NO_3$ and $N_2O_5$, the uncertainties are shown as error bars.

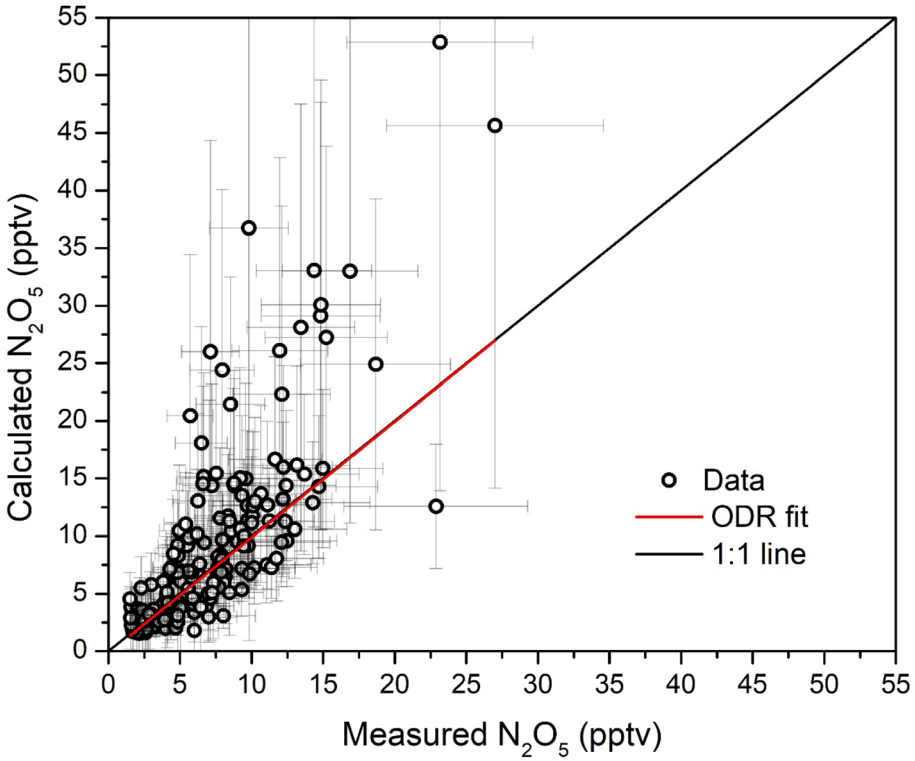


Fig. 5 $N_2O_5$ mixing ratios calculated from (Eq. 4) *versus* those directly measured. The red solid line shows an orthogonal distance regression (ODR,[57] slope: 1.00 ± 0.09, intercept: (−0.16 ± 0.34) pptv, Pearson correlation coefficient $r$ = 0.8) while the black line denotes ideal 1 : 1 agreement.

linear regression yields an intercept of (−0.16 ± 0.34) pptv and a slope of 1.00 ± 0.09, indicating very good agreement within associated uncertainties. As heterogeneous loss processes of both $N_2O_5$ and $NO_3$ are neglected in the calculation of $N_2O_5$ mixing ratios, and reactions of $NO_3$ with $RO_2$ (or other radicals) do not contribute to the measured loss term, we conclude that (within the associated uncertainty of this analysis), the loss of $NO_3$ (and thus indirectly $N_2O_5$) is dominated by reactions with VOCs and NO. The uptake of $N_2O_5$ to aqueous particles can be an important term outdoors, but in an indoor environments which is supplied with fresh-air *via* filters, particle concentrations indoors are too low for this to contribute significantly (see section 3.1). In addition, the RH was relatively low so that the water content of aerosol particles is expected to be minor, which lowers the $N_2O_5$ uptake coefficient.[52]

During period B (see Fig. 1, upper panel) a greater deviation between measured and calculated $N_2O_5$ mixing ratios is observed, which results in some of the scatter in Fig. 5. Period B is the only sunny period of the measurement period and an increase of 0.016 $s^{-1}$ in the $NO_3$ loss rate constant would be necessary to bring measured and calculated values into agreement. Such a reactivity would be caused by just 25 pptv of NO, which is below the LOD of the NO instrument.

### 3.3 Indoor fate of the nitrate radical

As indicated in section 1, reactions of $NO_3$ with VOCs may lead to $NO_x$ removal from the gas-phase, while reaction with NO leads to reformation of $NO_2$. Fig. 1 (panel d) suggests that the contribution of both reaction paths to $L_{NO_3}$ varies. We thus define the fractional contribution $F$ of $NO_3$ reactions with VOCs (represented by $k^{NO_3}$) to the overall $NO_3$ loss rate $L_{NO_3}$:

$$F = \frac{k^{NO_3}}{L_{NO_3}} = \frac{k^{NO_3}}{k^{NO_3} + k_3[NO]} \quad \text{(Eq. 5)}$$

The resulting fractional contributions are plotted together with measured (VOC-induced) $NO_3$ reactivities in Fig. 6. The mean fractional contribution of VOCs is 0.46 ± 0.31 (1σ). This implies that on average $NO_3$ was consumed roughly equally by NO and VOCs during the measurement period. It should be kept in mind that both the upper LOD of the $k^{NO_3}$ measurement and the lower LOD of the NO measurement bias the calculated fractional contributions to higher values (potential overestimation of $k^{NO_3}$ during NO-dominated periods and potential underestimation of NO-induced reactivity during VOC-dominated periods). During periods A–E, when $N_2O_5$ was above its LOD, the mean fractional contribution occasionally increased to 1, with a mean of 0.65 ± 0.32 (1σ). Both values are comparable to the nighttime outdoor values of 0.5–0.6 as observed at the summit of a semi-rural mountain site (impacted by both NO soil emissions and biogenic VOCs) *ca.* 30 km from the laboratory,[53] but lower than the values close to 1 as observed in forested regions where $NO_3$ reactivity is dominated by terpenes at night.[8,9] The closer agreement with nighttime

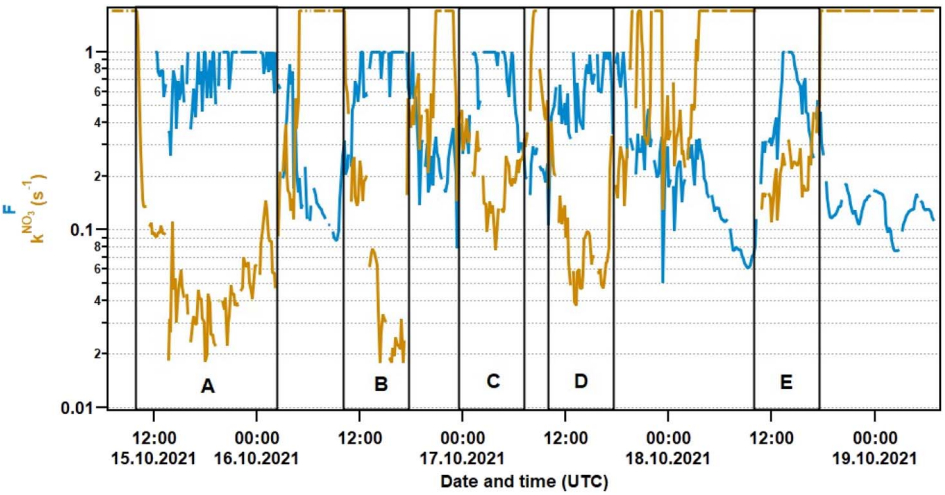


Fig. 6 $NO_3$ reactivity ($k^{NO_3}$) and fractional contribution F (Eq. 5) of $k^{NO_3}$ to the overall $NO_3$ loss rate $L_{NO_3}$.

outdoor conditions in urban environments is easily understood considering the lack of $NO_3$ photolysis and the abundance of $NO_x$ throughout the diel cycle. Moravek *et al.*[27] identified reaction with NO to be the dominant loss process in a highly-ventilated athletics facility during daytime, whereas the thermal equilibrium to $N_2O_5$ gained importance in the afternoon. Such a distinct diurnal variation is not observed in our short study.

Fig. 6 also shows that reaction with VOCs is a relevant $NO_3$ loss process most of the time in this particular environment. Unfortunately, there are no simultaneous VOC measurements available for this pilot study. Monoterpenes such as limonene are a class of organic compounds that are abundant in indoor environments due to their presence in detergents and cleaning agents[16,19,27] and which are highly reactive towards $NO_3$.[15] Terpenes or other unsaturated compounds released from indoor sources are thus the most likely organic reactants for $NO_3$. Reactive VOCs may however also originate from outside: the laboratory used in this study is located in the direct vicinity of deciduous trees, which at some times of the year can represent a significant source of isoprene as well as monoterpenes.[54–56] However, as our measurements were carried out in mid October with weak insolation and low temperatures, both of which result in low levels of biogenic activity, this is unlikely to represent the major source of indoor reactivity in this study.

## 4 Comparison to other indoor studies

In contrast to $O_3$ and OH, the nitrate radical has not been studied in indoor environments to a similar extent. Table 1 gives an overview of maximum mixing ratios of $NO_3$ (and $N_2O_5$) that were detected or modelled in different indoor environments.

As indicated in Fig. 1, up to 29 pptv of $N_2O_5$ were detected in our laboratory. The observation is comparable to 58 pptv of $N_2O_5$ + $NO_3$ (with $N_2O_5$ as the dominant fraction) that was observed inside an office building in Copenhagen, Denmark.[25] Note that both indoor environments were unoccupied, feature a comparable air change rate and are situated in urban areas. Arata *et al.*[26] reported 190 pptv of $N_2O_5$, if 40 ppbv $O_3$ was artificially added by a commercial ozone generator in order to force (together with 50–100 ppbv of $NO_2$) a very high $NO_3$ production rate of 7 ppbv $h^{-1}$. This is at least a factor of 10 higher than our

Table 1 Summary of studies on indoor measurements of $NO_3$ and $N_2O_5$[a]

| Reference | Environment | Method | Max. $NO_3/N_2O_5$ (pptv) | Air change rate ($h^{-1}$) |
|---|---|---|---|---|
| Carslaw[21] | Residential | Model calculation | 0.03 ($NO_3$) | 2 |
| Nøjgaard[25] | Office (Copenhagen) | Indirect measurement | 58 ($NO_3$ + $N_2O_5$) | 3.76 |
| Waring *et al.*[22] | Residential | Model calculation | 0.07 ($NO_3$) | 0.5 |
| Zhou *et al.*[13] | Residential (New York) | Steady-state calculation | $6.7 \times 10^{-4}$ ($NO_3$) | 0.65 |
| Arata *et al.*[26] | Residential (Oakland) | CRDS | 4 ($NO_3$) | 1–1.4 |
| Price *et al.*[23] | Museum (Boulder) | Steady-state calculation | 0.04 ($NO_3$) | 0.8 |
| Moravek *et al.* [27] | Athletic facility (Boulder) | CIMS | 4 ($N_2O_5$) | 7 |
| Link *et al.*[24] | Residential (Gaithersburg) | Model calculation | 0.3 ($NO_3$) | 0.24 |
| This study | Laboratory (Mainz) | CRDS ($N_2O_5$) | 29 ($N_2O_5$) | <4 |
| | | Steady-state calculation ($NO_3$) | 6 ($NO_3$) | |

[a] CRDS: Cavity ring-down spectroscopy, CIMS: chemical ionization mass spectrometry.

values of 0.04 to 0.2 pptv $s^{-1}$ for $P_{NO_3}$ and accounts for the lower $N_2O_5$ mixing ratios measured in our laboratory.

Recently, up to 4 pptv $N_2O_5$ (similar to our measurements in period C and E) were observed inside an athletics facility, which was not only more strongly ventilated (with an air change rate of 7 $h^{-1}$), but also occupied by humans.[27] In this case, $NO_3$ production rates between 0.025 and 0.3 pptv $s^{-1}$ are similar to ours, so the lower maximum $N_2O_5$ mixing ratio is a reflection of higher $NO_3$ loss rates of up to 8 $s^{-1}$ (at high-NO) compared to our median $L_{NO_3}$ of 0.15 $s^{-1}$.

In a study by Price *et al.*,[23] oxidation *via* $NO_3$ contributes ~10% to the total VOC loss in a museum that is ventilated with an air change rate of only 0.8 $h^{-1}$. The dominant loss process in this museum is ventilation with the residual contribution of 90%. Despite the fact that our air change rate is higher by a factor of 5, we estimated a higher $NO_3$ contribution of ~30% (see above). This discrepancy is explained by different indoor $NO_3$ levels: According to steady-state calculations, only 0.04 pptv $NO_3$ were present in the museum which is two orders of magnitudes lower compared to our values.

Link *et al.*[24] identified ventilation to be the dominant VOC sink (88%) in a residential building featuring an even lower air change rate and modelled $NO_3$ level of 0.2 $h^{-1}$ and 0.02 pptv, respectively. When 70 ppbv of $O_3$ were added artificially, oxidative processes competed with ventilation. In this case, ozonolysis (and OH production) drastically reduced the fractional contribution of (R7) to ~10%. Again, our higher fractional contribution of (R7) to the overall VOC loss is consequently reflected in our higher indoor $NO_3$ levels compared to those in Link *et al.*[24]

The $NO_3$ mixing ratios calculated from $NO_2$ and $N_2O_5$ mixing ratios (Fig. 1, panel e) are between 2 and 6 pptv and thus similar to the 3–4 pptv $NO_3$ that were directly measured in a residential kitchen[26] despite the great difference in $P_{NO_3}$. The comparable $NO_3$ levels are accordingly caused by the higher $NO_3$ reactivity of 0.8 $s^{-1}$ (calculated from VOC measurements) in the residential kitchen. In any case, mixing ratios of a few pptv clearly exceed indoor $NO_3$ levels predicted in model or steady-state calculations for residential environments by a factor of ~100.[13,21–24] This underlines the necessity of more direct measurements of $NO_3$ mixing ratios, $NO_3$ reactivity, the traces gases responsible for the loss of $NO_3$ and also the products (*e.g.* organic nitrates) of indoor $NO_3$–VOC interactions.

# 5 Conclusions

We present the first direct $NO_3$ reactivity measurement in a ventilated indoor environment. Our pilot study suggests that the nitrate radical concentration increases, when (1) indoor air is continuously exchanged with outdoor air so that both $O_3$ and $NO_2$ are available, (2) NO is (almost) entirely depleted by $O_3$ and (3) the room is not directly exposed to sunlight. A high ventilation rate (~4 $h^{-1}$) resulted in a high correlation between indoor and outdoor mixing ratios of $NO_2$ and $O_3$. Measured $N_2O_5$ and calculated $NO_3$ mixing ratios peaked at 29 and 6 pptv, which are significantly higher than reported in model calculations[21,22] but which agree with observations made in other ventilated (non-residential) rooms.[25,27] We demonstrate that, in indoor environments when highly polluted conditions impede the formation of detectable amounts of $NO_3$, measuring the $NO_3$ reactivity simultaneously with $NO_2$ and $O_3$ represents an alternative way to assess $NO_3$ mixing ratios. Furthermore, our $NO_3$ measurements emphasized the necessity of frequent inlet filter changes as common in outdoor field measurements. By comparing calculated with directly measured $NO_3$ reactivities, we find that the most important loss processes for $NO_3$ are reactions with NO and VOCs (such as monoterpenes), the latter thus providing an indoor source of organic nitrates. Direct $NO_3$ reactivity measurements can therefore contribute to identify the indoor fate of the nitrate radical.

# Author contributions

Patrick Dewald: conceptualization; data curation; formal analysis; investigation; methodology; visualization; writing – original draft; writing – review & editing. John N. Crowley: conceptualization; supervision; validation; writing – review & editing. Jos Lelieveld: resources; supervision; validation; writing – review & editing.

# Conflicts of interest

There are no conflicts to declare.

# Acknowledgements

We thank Chemours for provision of a FEP sample used to coat the flowtube reactor.

# References

1 N. E. Klepeis, W. C. Nelson, W. R. Ott, J. P. Robinson, A. M. Tsang, P. Switzer, J. V. Behar, S. C. Hern and W. H. Engelmann, The National Human Activity Pattern Survey (NHAPS): a resource for assessing exposure to environmental pollutants, *J. Exposure Anal. Environ. Epidemiol.*, 2001, **11**, 231–252.

2 C. J. Weschler, M. Brauer and P. Koutrakis, Indoor Ozone and Nitrogen-Dioxide - a Potential Pathway to the Generation of Nitrate Radicals, Dinitrogen Pentaoxide, and Nitric-Acid Indoors, *Environ. Sci. Technol.*, 1992, **26**, 179–184.

3 C. J. Weschler and H. C. Shields, Production of the hydroxyl radical in indoor air, *Environ. Sci. Technol.*, 1996, **30**, 3250–3258.

4 C. J. Young, S. Zhou, J. A. Siegel and T. F. Kahan, Illuminating the dark side of indoor oxidants, *Environ. Sci.: Processes Impacts*, 2019, **21**, 1229–1239.

5 N. Zannoni, P. S. J. Lakey, Y. Won, M. Shiraiwa, D. Rim, C. J. Weschler, N. J. Wang, L. Ernle, M. Z. Li, G. Bekö, P. Wargocki and J. Williams, The human oxidation field, *Science*, 2022, **377**, 1071–1076.

6 R. P. Wayne, I. Barnes, P. Biggs, J. P. Burrows, C. E. Canosamas, J. Hjorth, G. Lebras, G. K. Moortgat, D. Perner, G. Poulet, G. Restelli and H. Sidebottom, The

Nitrate Radical - Physics, Chemistry, and the Atmosphere, *Atmos. Environ.*, 1991, **25**, 1–203.

7 S. S. Brown and J. Stutz, Nighttime radical observations and chemistry, *Chem. Soc. Rev.*, 2012, **41**, 6405–6447.

8 J. Liebmann, E. Karu, N. Sobanski, J. Schuladen, M. Ehn, S. Schallhart, L. Quéléver, H. Hellen, H. Hakola, T. Hoffmann, J. Williams, H. Fischer, J. Lelieveld and J. N. Crowley, Direct measurement of $NO_3$ radical reactivity in a boreal forest, *Atmos. Chem. Phys.*, 2018, **18**, 3799–3815.

9 J. M. Liebmann, J. B. A. Muller, D. Kubistin, A. Claude, R. Holla, C. Plaß-Dülmer, J. Lelieveld and J. N. Crowley, Direct measurements of $NO_3$-reactivity in and above the boundary layer of a mountain-top site: Identification of reactive trace gases and comparison with OH-reactivity, *Atmos. Chem. Phys.*, 2018, **18**, 12045–12059.

10 A. Gandolfo, V. Gligorovski, V. Bartolomei, S. Tlili, E. G. Alvarez, H. Wortham, J. Kleffmann and S. Gligorovski, Spectrally resolved actinic flux and photolysis frequencies of key species within an indoor environment, *Build. Environ.*, 2016, **109**, 50–57.

11 S. Zhou and T. F. Kahan, Spatiotemporal characterization of irradiance and photolysis rate constants of indoor gas-phase species in the UTest house during HOMEChem, *Indoor Air*, 2022, **32**, e12964.

12 C. J. Weschler, Ozone in indoor environments: Concentration and chemistry, *Indoor Air*, 2000, **10**, 269–288.

13 S. Zhou, C. J. Young, T. C. VandenBoer, S. F. Kowal and T. F. Kahan, Time-Resolved Measurements of Nitric Oxide, Nitrogen Dioxide, and Nitrous Acid in an Occupied New York Home, *Environ. Sci. Technol.*, 2018, **52**, 8355–8364.

14 W. W. Nazaroff and C. J. Weschler, Indoor ozone: Concentrations and influencing factors, *Indoor Air*, 2022, **32**, e12942.

15 N. L. Ng, S. S. Brown, A. T. Archibald, E. Atlas, R. C. Cohen, J. N. Crowley, D. A. Day, N. M. Donahue, J. L. Fry, H. Fuchs, R. J. Griffin, M. I. Guzman, H. Herrmann, A. Hodzic, Y. Iinuma, J. L. Jimenez, A. Kiendler-Scharr, B. H. Lee, D. J. Luecken, J. Mao, R. McLaren, A. Mutzel, H. D. Osthoff, B. Ouyang, B. Picquet-Varrault, U. Platt, H. O. T. Pye, Y. Rudich, R. H. Schwantes, M. Shiraiwa, J. Stutz, J. A. Thornton, A. Tilgner, B. J. Williams and R. A. Zaveri, Nitrate radicals and biogenic volatile organic compounds: oxidation, mechanisms, and organic aerosol, *Atmos. Chem. Phys.*, 2017, **17**, 2103–2162.

16 W. W. Nazaroff and C. J. Weschler, Cleaning products and air fresheners: exposure to primary and secondary air pollutants, *Atmos. Environ.*, 2004, **38**, 2841–2865.

17 N. L. Ng, A. J. Kwan, J. D. Surratt, A. W. H. Chan, P. S. Chhabra, A. Sorooshian, H. O. T. Pye, J. D. Crounse, P. O. Wennberg, R. C. Flagan and J. H. Seinfeld, Secondary organic aerosol (SOA) formation from reaction of isoprene with nitrate radicals ($NO_3$), *Atmos. Chem. Phys.*, 2008, **8**, 4117–4140.

18 J. L. Fry, A. Kiendler-Scharr, A. W. Rollins, T. Brauers, S. S. Brown, H. P. Dorn, W. P. Dube, H. Fuchs, A. Mensah, F. Rohrer, R. Tillmann, A. Wahner, P. J. Wooldridge and R. C. Cohen, SOA from limonene: role of $NO_3$ in its generation and degradation, *Atmos. Chem. Phys.*, 2011, **11**, 3879–3894.

19 G. Bekö, P. Wargocki, N. J. Wang, M. Z. Li, C. J. Weschler, G. Morrison, S. Langer, L. Ernle, D. Licina, S. Yang, N. Zannoni and J. Williams, The Indoor Chemical Human Emissions and Reactivity (ICHEAR) project: Overview of experimental methodology and preliminary results, *Indoor Air*, 2020, **30**, 1213–1228.

20 N. Carslaw, L. Fletcher, D. Heard, T. Ingham and H. Walker, Significant OH production under surface cleaning and air cleaning conditions: Impact on indoor air quality, *Indoor Air*, 2017, **27**, 1091–1100.

21 N. Carslaw, A new detailed chemical model for indoor air pollution, *Atmos. Environ.*, 2007, **41**, 1164–1179.

22 M. S. Waring and J. R. Wells, Volatile organic compound conversion by ozone, hydroxyl radicals, and nitrate radicals in residential indoor air: Magnitudes and impacts of oxidant sources, *Atmos. Environ.*, 2015, **106**, 382–391.

23 D. J. Price, D. A. Day, D. Pagonis, H. Stark, L. B. Algrim, A. V. Handschy, S. Liu, J. E. Krechmer, S. L. Miller, J. F. Hunter, J. A. de Gouw, P. J. Ziemann and J. L. Jimenez, Budgets of Organic Carbon Composition and Oxidation in Indoor Air, *Environ. Sci. Technol.*, 2019, **53**, 13053–13063.

24 M. F. Link, J. Li, J. C. Ditto, H. Huynh, J. Yu, S. M. Zimmerman, K. L. Rediger, A. Shore, J. P. D. Abbatt, L. A. Garofalo, D. K. Farmer and D. Poppendieck, Ventilation in a Residential Building Brings Outdoor $NO_x$ Indoors with Limited Implications for VOC Oxidation from $NO_3$ Radicals, *Environ. Sci. Technol.*, 2023, **57**(43), 16446–16455.

25 J. K. Nøjgaard, Indoor measurements of the sum of the nitrate radical, $NO_3$, and nitrogen pentoxide, $N_2O_5$ in Denmark, *Chemosphere*, 2010, **79**, 898–904.

26 C. Arata, K. J. Zarzana, P. K. Misztal, Y. J. Liu, S. S. Brown, W. W. Nazaroff and A. H. Goldstein, Measurement of $NO_3$ and $N_2O_5$ in a Residential Kitchen, *Environ. Sci. Technol. Lett.*, 2018, **5**, 595–599.

27 A. Moravek, T. C. VandenBoer, Z. Finewax, D. Pagonis, B. A. Nault, W. L. Brown, D. A. Day, A. V. Handschy, H. Stark, P. Ziemann, J. L. Jimenez, J. A. de Gouw and C. J. Young, Reactive Chlorine Emissions from Cleaning and Reactive Nitrogen Chemistry in an Indoor Athletic Facility, *Environ. Sci. Technol.*, 2022, **56**, 15408–15416.

28 Y. Shah, J. W. Kurelek, S. D. Peterson and S. Yarusevych, Experimental investigation of indoor aerosol dispersion and accumulation in the context of COVID-19: Effects of masks and ventilation, *Phys. Fluids*, 2021, **33**, 073315.

29 R. A. Cox, M. Ammann, J. N. Crowley, P. T. Griffiths, H. Herrmann, E. H. Hoffmann, M. E. Jenkin, V. F. McNeill, A. Mellouki, C. J. Penkett, A. Tilgner and T. J. Wallington, Opinion: The germicidal effect of ambient air (open-air factor) revisited, *Atmos. Chem. Phys.*, 2021, **21**, 13011–13018.

30 M. H. Sherman, Tracer-Gas Techniques for Measuring Ventilation in a Single Zone, *Build. Environ.*, 1990, **25**, 365–374.

31 J. M. Liebmann, G. Schuster, J. B. Schuladen, N. Sobanski, J. Lelieveld and J. N. Crowley, Measurement of ambient $NO_3$ reactivity: Design, characterization and first deployment of a new instrument, *Atmos. Meas. Tech.*, 2017, **10**, 1241–1258.

32 N. Sobanski, J. Schuladen, G. Schuster, J. Lelieveld and J. N. Crowley, A five-channel cavity ring-down spectrometer for the detection of $NO_2$, $NO_3$, $N_2O_5$, total peroxy nitrates and total alkyl nitrates, *Atmos. Meas. Tech.*, 2016, **9**, 5103–5118.

33 N. Friedrich, I. Tadic, J. Schuladen, J. Brooks, E. Darbyshire, F. Drewnick, H. Fischer, J. Lelieveld and J. N. Crowley, Measurement of NOx and NOy with a thermal dissociation cavity ring-down spectrometer (TD-CRDS): instrument characterisation and first deployment, *Atmos. Meas. Tech.*, 2020, **13**, 5739–5761.

34 J. B. Burkholder, S. P. Sander, J. Abbatt, J. R. Barker, R. E. Huie, C. E. Kolb, M. J. Kurylo, V. L. Orkin, D. M. Wilmouth and P. H. Wine, *Chemical Kinetics and Photochemical Data for Use in Atmospheric Studies, Evaluation No. 18*, JPL Publication 15-10, Jet Propulsion Laboratory, Pasadena, **https://jpldataeval.jpl.nasa.gov**, accessed 23 July 2023.

35 IUPAC, *Task Group on Atmospheric Chemical Kinetic Data Evaluation*, ed. M. Ammann, R. A. Cox, J. N. Crowley, H. Herrmann, M. E. Jenkin, V. F. McNeill, A. Mellouki, M. J. Rossi, J. Troe and T. J. Wallington, **https://iupac.aeris-data.fr/en/home-english/**, accessed 23 July 2023.

36 M. J. Tang, J. Thieser, G. Schuster and J. N. Crowley, Uptake of $NO_3$ and $N_2O_5$ to Saharan dust, ambient urban aerosol and soot: a relative rate study, *Atmos. Chem. Phys.*, 2010, **10**, 2965–2974.

37 G. Schuster, I. Labazan and J. N. Crowley, A cavity ring down/cavity enhanced absorption device for measurement of ambient $NO_3$ and $N_2O_5$, *Atmos. Meas. Tech.*, 2009, **2**, 1–13.

38 *Umweltbundesamt*, **https://www.umweltbundesamt.de/en/data/air/air-data/**, accessed 12 June 2023.

39 Y. Hu and B. Zhao, Relationship between indoor and outdoor $NO_2$: A review, *Build. Environ.*, 2020, **180**, 106909.

40 T. Grontoft, The influence of photochemistry on outdoor to indoor $NO_2$ in some European museums, *Indoor Air*, 2022, **32**, e12999.

41 J. N. Crowley, G. Schuster, N. Pouvesle, U. Parchatka, H. Fischer, B. Bonn, H. Bingemer and J. Lelieveld, Nocturnal nitrogen oxides at a rural mountain site in south-western Germany, *Atmos. Chem. Phys.*, 2010, **10**, 2795–2812.

42 U. F. Platt, A. M. Winer, H. W. Biermann, R. Atkinson and J. N. Pitts, Measurement of Nitrate Radical Concentrations in Continental Air, *Environ. Sci. Technol.*, 1984, **18**, 365–369.

43 F. Heintz, U. Platt, H. Flentje and R. Dubois, Long-term observation of nitrate radicals at the tor station, Kap Arkona (Rügen), *J. Geophys. Res.: Atmos.*, 1996, **101**, 22891–22910.

44 M. Martinez, D. Perner, E. M. Hackenthal, S. Kulzer and L. Schutz, $NO_3$ at Helgoland during the NORDEX campaign in October 1996, *J. Geophys. Res.: Atmos.*, 2000, **105**, 22685–22695.

45 S. S. Brown, H. Stark, T. B. Ryerson, E. J. Williams, D. K. Nicks, M. Trainer, F. C. Fehsenfeld and A. R. Ravishankara, Nitrogen oxides in the nocturnal boundary layer: Simultaneous in situ measurements of $NO_3$, $N_2O_5$, $NO_2$, NO, and $O_3$, *J. Geophys. Res.: Atmos.*, 2003, **108**, 4299.

46 S. S. Brown, J. A. Degouw, C. Warneke, T. B. Ryerson, W. P. Dube, E. Atlas, R. J. Weber, R. E. Peltier, J. A. Neuman, J. M. Roberts, A. Swanson, F. Flocke, S. A. McKeen, J. Brioude, R. Sommariva, M. Trainer, F. C. Fehsenfeld and A. R. Ravishankara, Nocturnal isoprene oxidation over the Northeast United States in summer and its impact on reactive nitrogen partitioning and secondary organic aerosol, *Atmos. Chem. Phys.*, 2009, **9**, 3027–3042.

47 N. Sobanski, M. J. Tang, J. Thieser, G. Schuster, D. Pöhler, H. Fischer, W. Song, C. Sauvage, J. Williams, J. Fachinger, F. Berkes, P. Hoor, U. Platt, J. Lelieveld and J. N. Crowley, Chemical and meteorological influences on the lifetime of $NO_3$ at a semi-rural mountain site during PARADE, *Atmos. Chem. Phys.*, 2016, **16**, 4867–4883.

48 S. S. Brown, H. Stark and A. R. Ravishankara, Applicability of the steady state approximation to the interpretation of atmospheric observations of $NO_3$ and $N_2O_5$, *J. Geophys. Res.: Atmos.*, 2003, **108**, 4539.

49 P. Dewald, J. M. Liebmann, N. Friedrich, J. Shenolikar, J. Schuladen, F. Rohrer, D. Reimer, R. Tillmann, A. Novelli, C. M. Cho, K. M. Xu, R. Holzinger, F. Bernard, L. Zhou, W. Mellouki, S. S. Brown, H. Fuchs, J. Lelieveld and J. N. Crowley, Evolution of $NO_3$ reactivity during the oxidation of isoprene, *Atmos. Chem. Phys.*, 2020, **20**, 10459–10475.

50 C. J. Weschler and H. C. Shields, Measurements of the hydroxyl radical in a manipulated but realistic indoor environment, *Environ. Sci. Technol.*, 1997, **31**, 3719–3722.

51 N. Carslaw, A mechanistic study of limonene oxidation products and pathways following cleaning activities, *Atmos. Environ.*, 2013, **80**, 507–513.

52 T. H. Bertram and J. A. Thornton, Toward a general parameterization of $N_2O_5$ reactivity on aqueous particles: the competing effects of particle liquid water, nitrate and chloride, *Atmos. Chem. Phys.*, 2009, **9**, 8351–8363.

53 P. Dewald, C. M. Nussbaumer, J. Schuladen, A. Ringsdorf, A. Edtbauer, H. Fischer, J. Williams, J. Lelieveld and J. N. Crowley, Fate of the nitrate radical at the summit of a semi-rural mountain site in Germany assessed with direct reactivity measurements, *Atmos. Chem. Phys.*, 2022, **22**, 7051–7069.

54 C. Calfapietra, S. Fares, F. Manes, A. Morani, G. Sgrigna and F. Loreto, Role of Biogenic Volatile Organic Compounds (BVOC) emitted by urban trees on ozone concentration in cities: A review, *Environ. Pollut.*, 2013, **183**, 71–80.

55 E. C. Lahr, G. W. Schade, C. C. Crossett and M. R. Watson, Photosynthesis and isoprene emission from trees along an

urban–rural gradient in Texas, *Global Change Biol.*, 2015, **21**, 4221–4236.
56 Y. Gao, M. Ma, F. Yan, H. Su, S. Wang, H. Liao, B. Zhao, X. Wang, Y. Sun, J. R. Hopkins, Q. Chen, P. Fu, A. C. Lewis, Q. Qiu, X. Yao and H. Gao, Impacts of biogenic emissions from urban landscapes on summer ozone and secondary organic aerosol formation in megacities, *Sci. Total Environ.*, 2022, **814**, 152654.
57 D. York, Least-Squares Fitting of a Straight Line, *Can. J. Phys.*, 1966, **44**, 1079–1086.